Journal of Industrial and Engineering Chemistry 80 (2019) 471–478

Contents lists available at ScienceDirect

Journal of Industrial and Engineering Chemistry

journal homepage: www.elsevier.com/locate/jiec

Fabrication of microgrooved scaffolds using near-field electrospinning-assisted lithography (NFEAL)

SungYeun Yang[a,1], Ji Hong Min[b,c,1], Kanghee Cho[b], Il Ho Seo[a], WonHyoung Ryu[a,*], Won-Gun Koh[b,*]

[a] Department of Mechanical Engineering, Yonsei University, Yonsei-ro 50, Seodaemun-gu, Seoul 03722, Republic of Korea
[b] Department of Chemical and Biomolecular Engineering, Yonsei University, Yonsei-ro 50, Seodaemun-gu, Seoul 03722, Republic of Korea
[c] Active Polymer Center for Pattern Integration (APCPI), Yonsei-ro 50, Seodaemun-gu, Seoul 03722, Republic of Korea

ARTICLE INFO

Article history:
Received 13 June 2019
Received in revised form 4 July 2019
Accepted 7 August 2019
Available online 27 August 2019

Keywords:
Near-field electrospinning-assisted lithography
Microgrooved substrate
Cell alignment
Topographical guidance
Tissue engineering

ABSTRACT

A simple patterning process combining near-field electrospinning (NFE) and template lithography, called near-field electrospinning-assisted lithography (NFEAL), was developed to prepare polymeric scaffolds with microgroove patterns for potential use in biomedical applications. NFE enabled the deposition of poly (ethylene oxide) (PEO) fibers at a desired position. The diameters of the deposited PEO fibers could be controlled over a range of 0.5–20 μm by adjusting the NFE parameters such as voltage, distance, feed rate, and translation speed. The preparation of PEO fibers with 1 and 3 μm diameters using NFE, followed by the deposition of polystyrene (PS) and removal of the fiber template, created free-standing PS scaffolds with microgroove patterns. The width of the microgroove was similar to the diameter of the PEO fibers. The depth of the microgroove was also dependent on the dimensions of the PEO fibers; microgrooves of depth 64.49 ± 11.5 nm and 216.68 ± 62.9 nm were fabricated from PEO fibers of diameters 1 and 3 μm, respectively. When C2C12 cells were cultured on the microgrooved scaffolds, they showed enhanced elongation or alignment along the microgrooved scaffolds, especially, for the microgroove (1 μm) with a smaller width.

Introduction

Near-field electrospinning (NFE) is a technique that overcomes the problem of randomness in conventional electrospun fibers. This technique utilizes only the stable jet zone by maintaining a very short distance between the metal needle and the grounded substrate, where a low voltage is applied during electrospinning [1–3]. It is similar to electrohydrodynamics (EHD) in that the solution can be deposited at the desired location; however, in NFE, nondroplet fibers are continuously deposited in line. NFE is a simple, but powerful, strategy capable of directly depositing nano or micrometer-scale fibers, with excellent controllability. The pattern resolutions of NFE are comparable to those achieved by conventional lithography techniques that are much more complex and expensive. Deposition of nano/microscale fibers with the desired thickness, spacing, and material properties, at specific locations, is very useful, and expands the application areas of NFE to cover optical devices, nanogenerators, wearable sensors, tissue engineering, drug delivery, and nano/microelectromechanical systems [4–15]. Thus far, the majority of the NFE-related studies presented the generation of various fiber patterns and the direct use of the deposited nano/microfibers [1–3,16–21]. Because most of the fiber patterns were generated on rigid and conductive substrates, it was impossible to use the fiber-pattern–containing substrates in a free-standing form such as in implantable biomedical scaffolds.

In this study, we introduce a very simple technique that is capable of generating groove patterns with submicrometer-scale widths (1–10 μm) using fibers deposited by NFE, which we call NFE-assisted lithography (NFEAL). NFEAL is capable of fabricating various groove patterns using deposited nano/micropatterns as sacrificial templates. Conventionally, various nano/micro printing techniques have been utilized to produce nano/microgroove patterns [22–27]. However, these techniques have certain limitations such as the high cost of synthesizing the master mold by lithography and the requirement of additional steps, which may need additional heat, pressure, and/or light sources. NFEAL is an economic and simple technique that can create high-resolution groove patterns on various polymeric substrates. In this work, we

* Corresponding authors.
E-mail addresses: whryu@yonsei.ac.kr (W. Ryu), wongun@yonsei.ac.kr (W.-G. Koh).
[1] These authors contributed equally to this work.

https://doi.org/10.1016/j.jiec.2019.08.025
1226-086X/

chose poly(ethylene oxide) (PEO) as the fiber material and polystyrene (PS) as the scaffold material. Three simple steps—deposition of PEO fiber by NFE, pouring PS solution onto the PEO fiber patterns, and subsequent removal of PEO fibers with nontoxic solvents such as water—generated PS scaffolds with submicrometer-wide microgrooves. After controlling the diameters of the PEO fibers, which determine the width of the microgrooves, and confirming the successful transfer of the fiber patterns to the microgroove, we investigated the possibility of using the developed scaffolds as a new platform for the topographical guidance of C2C12 myoblast cells by evaluating the effects of the microgroove patterns on the directional growth and elongation of the C2C12 cells.

Materials and methods

Preparation of solution

The solutions used in NFE were prepared by dissolving PEO (Sigma-Aldrich, USA) with molecular weight (MW) 900,000 in deionized (DI) water, at a concentration of 5 wt.%. For the substrate, PS (Sigma-Aldrich, USA) with molecular weight 192,000 was dissolved in Tetrahydrofuran (THF, Samchun Industry Ltd, South Korea), at a concentration of 20 wt.%.

Near-field electrospinning

The NFE system was set up by adding the x-axis stage to the electrospinning apparatus (NanoNC, South Korea, ESR200RD). The setup consisted of a high-voltage power supply, syringe pump, y-axis moving metal nozzle, and X-axis stage (Fig. 1). The PEO solution was fed to the metal nozzle by a syringe pump at a rate of 0.5–10 μL/min. Voltages ranging from 0.8 to 2.0 kV were supplied to the nozzle by the power supply. The needle-to-substrate distance was in the range of 1–3 mm, and the substrate was connected to the ground. The nozzle moved with a step distance of 10–150 μm at various speeds ranging from 500 to 10,000 mm/min, in the x-direction, and the substrate moved 1.5–2.0 cm in the y-direction at the same speed as that of the nozzle movement in the x-direction. To determine the relation between the fiber diameter and NFE parameters, the NFE conditions such as the voltage, distance, translation speed, and feed rate were controlled. When one parameter was varied, the values of the other variables remained fixed.

Preparation of patterned PS substrate

Fig. 1 also shows the process for the generation of a patterned PS substrate using NFE (we call this process NFEAL). The homogeneously dissolved PS solution was poured on the as-prepared PEO fiber patterns and dried for 12 h in a hood. The patterned PS substrate was obtained by detaching the PEO-fiber-embedded PS from the substrate, and subsequently, dissolving the PEO fiber patterns in water. The diameter of the PEO fiber, which would be the width of the pattern on the PS substrate, was controlled by changing the NFE operating conditions. The morphology of the patterned PS substrate was observed using scanning electron microscopy (SEM) (JEOL-7001F, JEOL, Japan). The generation of

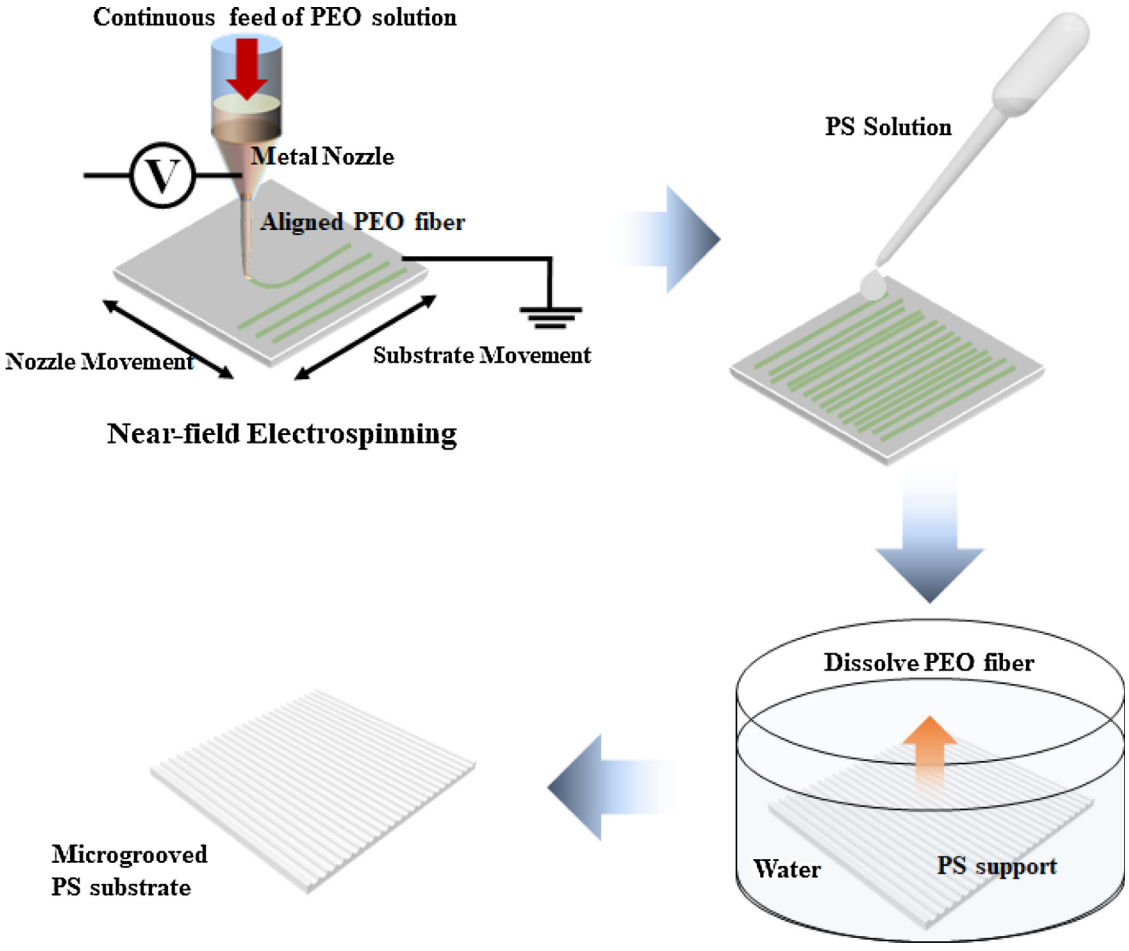

Fig. 1. Schematic illustration of preparing microgrooved polymeric substrate using NFEAL.

patterns on the PS substrate was confirmed with a surface profiler (DektakXT, Bruker, USA) with a stylus force of 6.5 mg and radius 2 μm.

Cell culture and seeding

C2C12 mouse myoblast cells were chosen to determine the degree of cell elongation according to the aligned pattern of the substrate, because the C2C12 cell body responds sensitively to the effects of surface topography [28–31]. The C2C12 myoblast cell lines, derived from a mouse heart (Korea Cell Line Bank, Korea), were cultured in RPMI 1640 medium (Invitrogen, US) containing 10% fetal bovine serum and 1% penicillin/streptomycin solution. The cells were then incubated at 37 °C in 5% CO_2 and 95% air. Cells were seeded onto the microgrooved PS substrate after they were trypsinized and centrifuged at 1200 rpm at 25 °C for five minutes. After removing the supernatant, the cells were re-suspended in RPMI medium containing serum. A 10 μL aliquot was used to determine cell density in a hemocytometer. Finally, approximately 1.0×10^4 cells were seeded onto the patterned substrate for cell studies. The PS substrates were coated with poly (L-Lysine) (PLL, Sigma-Aldrich, USA) prior to cell seeding to facilitate cell adhesion [32]. After five hours, the cell-seeded PS substrates were placed to new 24-well plates to eliminate the effects of the cells that adhered to the well plate. The cell culture media were replaced every day.

Cell analysis

Cell proliferation and viability assay

The proliferation of the adhered cells was investigated using (3-(4,5-dimethylthiazol-2-yl)-2,5-diphenyltetrazolium bromide (MTT) (Sigma-Aldrich, USA) assays. In brief, a 10% (v/v) MTT solution (5 mg/ml) was added to the sample-containing culture medium. The samples were reacted at 37.8 °C for one hour and the formazan crystals transformed from the MTT solution by mitochondrial reductase were dissolved in DMSO. The absorbance of these samples was measured at 540 nm using a microplate reader (Molecular Devices, Sunnyvale, CA, USA). The cells attached to the supports were observed with Live/Dead Viability/Cytotoxicity fluorescence assay. After the C2C12 seeded substrate was washed twice with DPBS, the media of the PS support samples were immersed in a solution containing 0.2% (v/v) calcein AM and 0.05% (v/v) ethidium homodimer (ethD-1) (Invitrogen, US) in DPBS solution. After incubation for an hour at 37.8 °C, the samples were placed to new 24-well plates and washed twice with DPBS to remove any debris. The live/dead

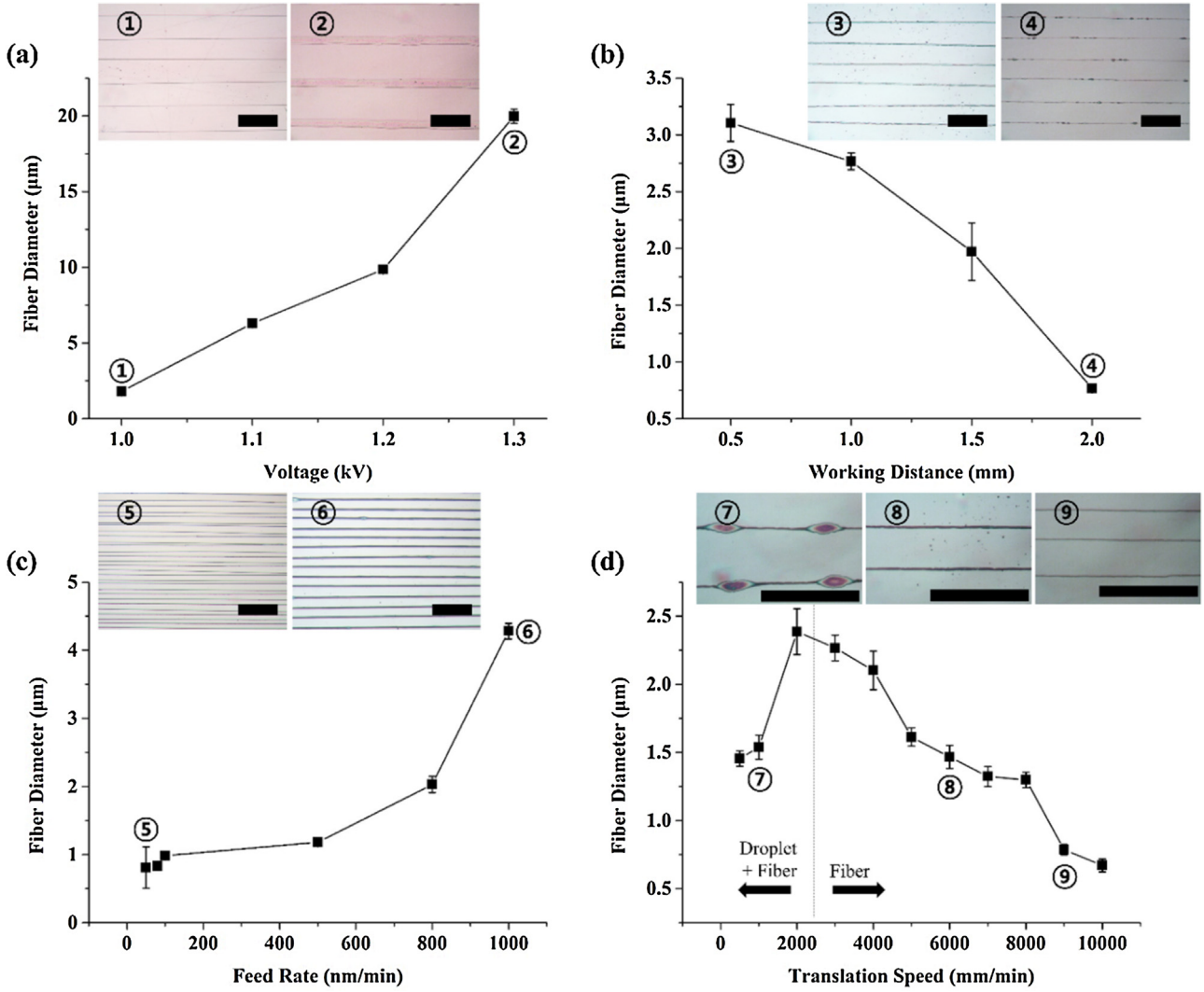

Fig. 2. Optical images and plots of fiber diameter according to NFE parameterss such as (a) voltage, (b) working distance, (c) feed rate, and (d) translation speed. Scale bars of insets are 100 μm.

images were observed using an inverted fluorescence microscope (IX53, Olympus Corp., Japan).

FITC-phalloidin and DAPI staining

Fluorescence staining was performed using fluorescein isothiocyanate (FITC)-conjugated phalloidin (Invitrogen, US), and nuclear staining with DAPI (Invitrogen, US). C2C12 cells were fixed with 4% paraformaldehyde for 20 min at room temperature and washed twice with DPBS. Then, 10 μL of 6 μM stock solution of FITC-phalloidin and 500 μL of DPBS were added to the PS substrates with different pattern sizes in the 24-well plates, at room temperature for one hour. After washing twice with DPBS, 5 μL of 10 μM stock solution of DAPI and 500 μL of DPBS were added to the PS substrate at room temperature for two minutes. Next, the samples were washed twice with DPBS. The stained samples were subjected to fluorescence imaging using an inverted fluorescence microscope.

Cell orientation and elongation

To observe the shape and alignment of the cell body, in the SEM images, the cultured cells on the substrates were fixed with 4% paraformaldehyde for 20 min at room temperature and washed twice with DPBS. After that, the substrates were sterilized in 30, 50, and 70% (v/v) ethanol solutions for five minutes each. The orientation and elongation of the cells were investigated using inverted fluorescence microscope (IX53, Olympus Corp., Japan) and analyzed using ImageJ software. The elongation of the C2C12 cells on the patterned PS substrates was quantitatively measured in terms of the aspect ratio, which is the ratio between the length of the longest line and the shortest line, across the nuclei. The orientations of the cells were evaluated from the FITC-phalloidin fluorescence images by angle measurement between the long axis of the cells and the microgroove direction on the support, to make a histogram.

Results and discussion

Parametric control of NFE

Experiments were conducted by controlling one parameter while the other parameters were fixed. For each test, the fixed values were 1 kV voltage, 32 G needle, 1 mm distance, 100 nL/min feed rate, and 4000 mm/min translation speed. The voltage was increased from 1.0 kV to 1.3 kV in steps of 0.1 kV. As the voltage increased, the charge density in the meniscus increased, which increased the diameter of the PEO fiber. The fiber diameter changed from 1.8 ± 0.06 to 19.9 ± 0.5 μm (Fig. 2a). Increase in the distance tended to increase the flight time of the electrospun fibers. This led to increased stretching of the fiber, which was induced by an internal repulsive force. As a result, the PEO fibers became thinner as the distance increased. The fiber diameters changed from 3.1 ± 0.1 to 0.8 ± 0.03 μm (Fig. 2b). The feed rate was also known to regulate the fiber diameter; higher feed rates resulted in larger fiber diameters. The fiber diameter increased from 0.8 ± 0.3 μm at 50 nL/min to 4.3 ± 0.1 μm at 1000 nL/min (Fig. 2c). In NFE, the translation speed, which is the speed of the substrate while depositing NFE fibers, also influences the fiber pattern significantly. When the translation speed was slower than the speed of fiber deposition, which was true for translation speeds below 3000 mm/min, jetted fibers piled up on the substrate or beads were formed (Fig. 2d). When the translation speed was above 4000 mm/min, the deposited fibers were stretched and became thin. The fiber diameters ranged between 1.5 ± 0.1 and 2.4 ± 0.03 μm below 3000 mm/min with beads along the fibers,

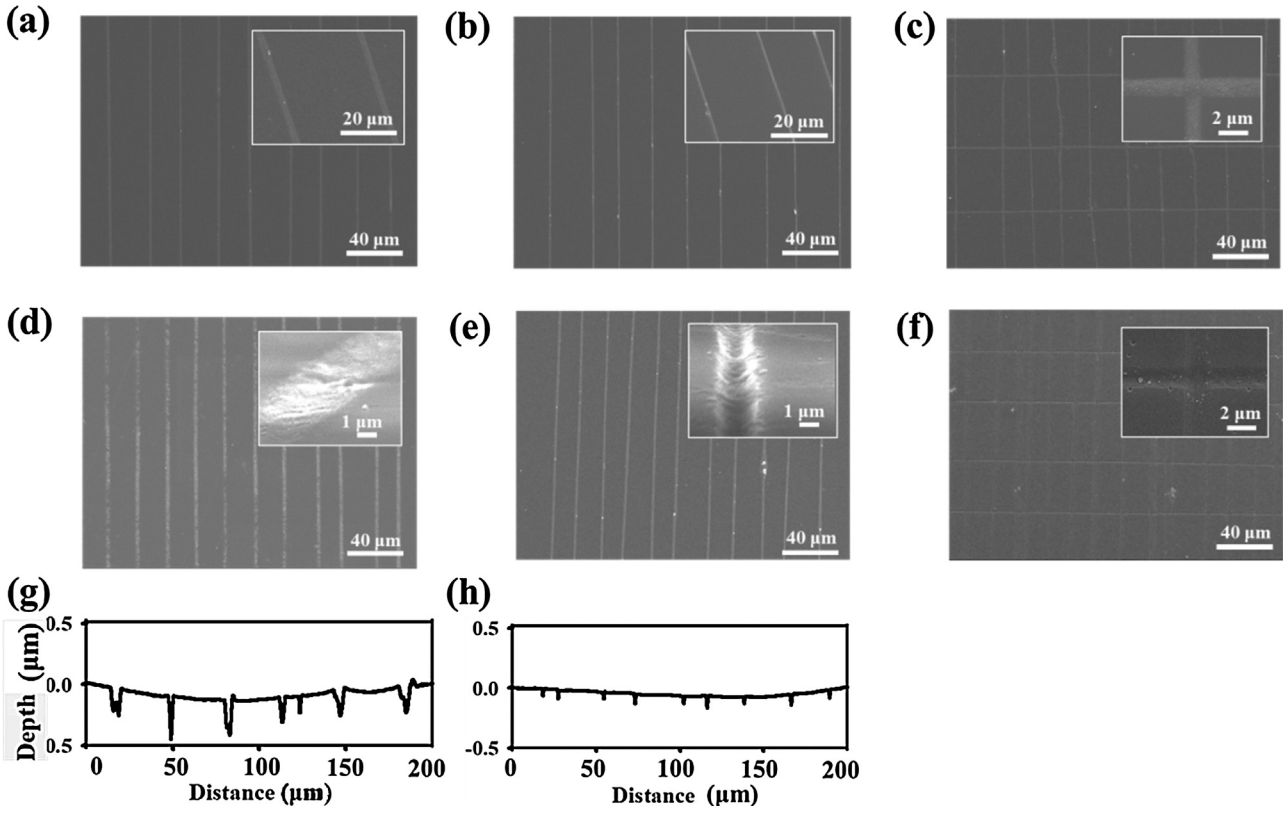

Fig. 3. SEM images of PEO fibers. Aligned PEO fibers with (a) 1 μm and (b) 3 μm diameter, (c) grid pattern of PEO fibers. SEM images of PS substrates with (d) 1 μm microgroove, (e) 3 μm microgroove, and (f) grid pattern. Surface profiles of PS substrate obtained from (g) 1 μm microgroove and (h) 3 μm microgroove.

and they decreased from 2.3 0.05 m at 4,000 mm/ min to 0.7 0.4 ± 0.05 μm at 4000 mm/min to 0.7 ± 0.4 μm at 10,000 mm/min.

Fabrication of patterned PS substrate

Patterned substrates were obtained by casting a PS solution on a PEO-fiber–deposited surface and the subsequent removal of the PEO fiber, as described in Fig. 1. We called this process NFEAL. As shown in Fig. 3a–f, the PEO aligned fiber-based templates were transferred to the PS substrate as groove patterns with submicrometer widths. The widths and intervals of each sample group are summarized in Table 1. The width of the groove was determined by the diameter of the PEO fibers, which was controlled by various NFE variables, as demonstrated in Fig. 2. In this study, we prepared the aligned groove patterns using PEO fibers of diameters 1 μm and 3 μm (Fig. 3a and b). These patterns were replicated as aligned grooves with widths of 1.05 ± 0.29 μm (Fig. 3d) and 3.11 ± 0.10 μm (Fig. 3e), respectively (we call these PS substrates with groove patterns as 1 μm microgroove and 3 μm microgroove, respectively). The interval of each aligned groove pattern in the PS substrate was 20.45 ± 3.1 μm and 23.26 ± 4.5 μm for the 1 μm and 3 μm microgroove, respectively (Fig. 3d and e). The depths of the PS microgrooves were measured with a surface profiler (Fig. 3g & h). The pattern depth was 64.49 ± 11.5 nm and 216.68 ± 62.9 nm for 1 μm and 3 μm microgroove, respectively. To further verify the pattern transformation of NFEAL, we fabricated a grid PEO-fiber–patterned NFE, as shown in Fig. 3c. The same PS casting and PEO removal techniques mentioned above were used to create grid microgroove patterns on PS substrates (Fig. 3f). The fiber width of this sample was 1 μm, and the spacing along the x-axis and y-axis were 23.26 ± 4.5 μm and 40.23 ± 2.5 μm, respectively. The SEM image confirmed that the structure was transferred with high replication accuracy.

Cell viability and proliferation

The cell adhesion and proliferation on the microgrooved PS substrates were investigated using the MTT assay (Fig. 4). PS substrates were coated with PLL to enhance cell adhesion [33]. The PLL coating did not affect the morphology of the microgroove patterns on the PS support. The MTT assay results indicated that the C2C12 cells were viable and proliferated on the three different PLL-coated PS substrates, as shown in Fig. 4a. The adhered cells were visualized using a Live/Dead Viability/Cytotoxicity fluorescence assay that stained the live cells green and dead cells red. As shown in the fluorescence images in Fig. 4b, all the adhered cells on different substrates emitted green fluorescence, indicating that the cells remained viable on the substrates.

Cellular alignment and elongation in patterned substrates

The C2C12 myoblasts were cultured and monitored on the microgrooved PS substrates for three days. The changes in the cell morphology, resulting from the groove patterns, were first studied with fluorescence images (Fig. 5). On both microgrooves, the cells were elongated in the pattern direction, demonstrating that the microgrooves fabricated using NFEAL could guide cell growth and orientation through pattern alignment.

Table 1
The dimensions of two different microgrooved PS substrate.

Sample name	Pattern width	Pattern interval	Pattern depth
1 μm microgroove	1.05 ± 0.29 μm	20.45 ± 3.1 μm	64.49 ± 11.5 nm
3 μm microgroove	3.11 ± 0.10 μm	23.26 ± 4.5 μm	216.68 ± 62.9 nm

The quantitative analysis of C2C12 cell elongation on microgrooved substrates was performed by measuring the cellular aspect ratio (A/R) after three days of culture. The A/R was determined as the ratio between the lengths of the longest line and shortest line of the cell body, using FITC-phalloidin fluorescence images (Fig. 6) [34]. On plain PS substrate without microgroove, the A/R of the cells was 2.5, while the A/R was 3.9 and 7.2 for the cells cultured on the substrates with 1 and 3 μm microgroove, respectively (Fig. 6a). In particular, the average A/R of the C2C12 cell body cultured in the PS substrate with 1 μm microgroove was higher than that of the cells cultured in the PS substrate with 3 μm microgroove. This indicated that narrower microgrooves could induce higher degrees of cell elongation.

The degree of cell alignment was also estimated by measuring the angle between the longest part of each myoblast and the pattern direction, using ImageJ (Fig. 6b–d). The angle of the C2C12 cells parallel to the patterns was set as 0° and the angle of the C2C12 cells perpendicular to the patterns was set to 90°. The cells cultured on a plain substrate did not have any preferential angle of alignment (Fig. 6b). Meanwhile, the cells grown on the substrates with microgrooves had narrower distributions of orientation angles, centered at 0° ± 10° (Fig. 6c & d). When the cells were cultured on the 1 μm microgroove, the cell elongation angle showed much narrower distribution than that of the cells cultured on the 3 μm microgroove (Fig. 6d).

Further discussions

Electrospinning is widely used to create nano or submicrometer-scale fibrous structures and many studies are developing new methods to implement this technique on nano/microdevices [35–38]. However, electrospinning does not allow the deposition of individual fibers, with high accuracy, by adjusting the process parameters. NFE can overcome this limitation of the electrospinning process. Thus, the near-field electrospinning (NFE) process was developed to directly write orderly nano/microfibers, whose diameters and morphology can be controlled easily by changing the various NFE process variables [3,13,15–17,19,39]. Beyond the deposition of fibrous structures in a well-controlled manner, we further attempted to use directly-written PEO fiber structures as sacrificial templates, where well-defined microgroove PS patterns were obtained after the deposition and subsequent removal of the sacrificial fibers.

Because the geometry of the microgroove was determined by the sacrificial fiber that was controlled by the NFE, we first controlled the diameter of the PEO fiber by changing various factors. Fig. 2 shows that the fiber diameter could be controlled by several parameters such as voltage, working distance, feed rate, and translation speed. Although the fiber diameter could be tuned within the range of 1 μm–20 μm, we chose 1 μm and 3 μm fibers for application to the topographical guidance of C2C12 cell alignment and oriented growth, as most cells were distinctly aligned for groove widths narrower than the cell diameter in suspension (10–20 μm). Since this process is in nature electrospinning, the pattern can be as small as 100 nm with the change of ink solution properties. The distance between the microgrooves could be made as small as 10 um. However, with 10 um distance, the larger area patterning becomes more difficult due to vibration of the translation stage when it changes the moving direction. Further reduction of the distance is possible by using a higher-precision motion stage system.

Because of the insolubility of PEO to PS solution in THF and insolubility of PS to water, pouring PS solution onto PEO fiber patterns and dissolving the PEO fiber pattern with water did not cause any damage, which allowed the fabrication of PS substrates with well-defined submicrometer-sized groove patterns (Fig. 3).

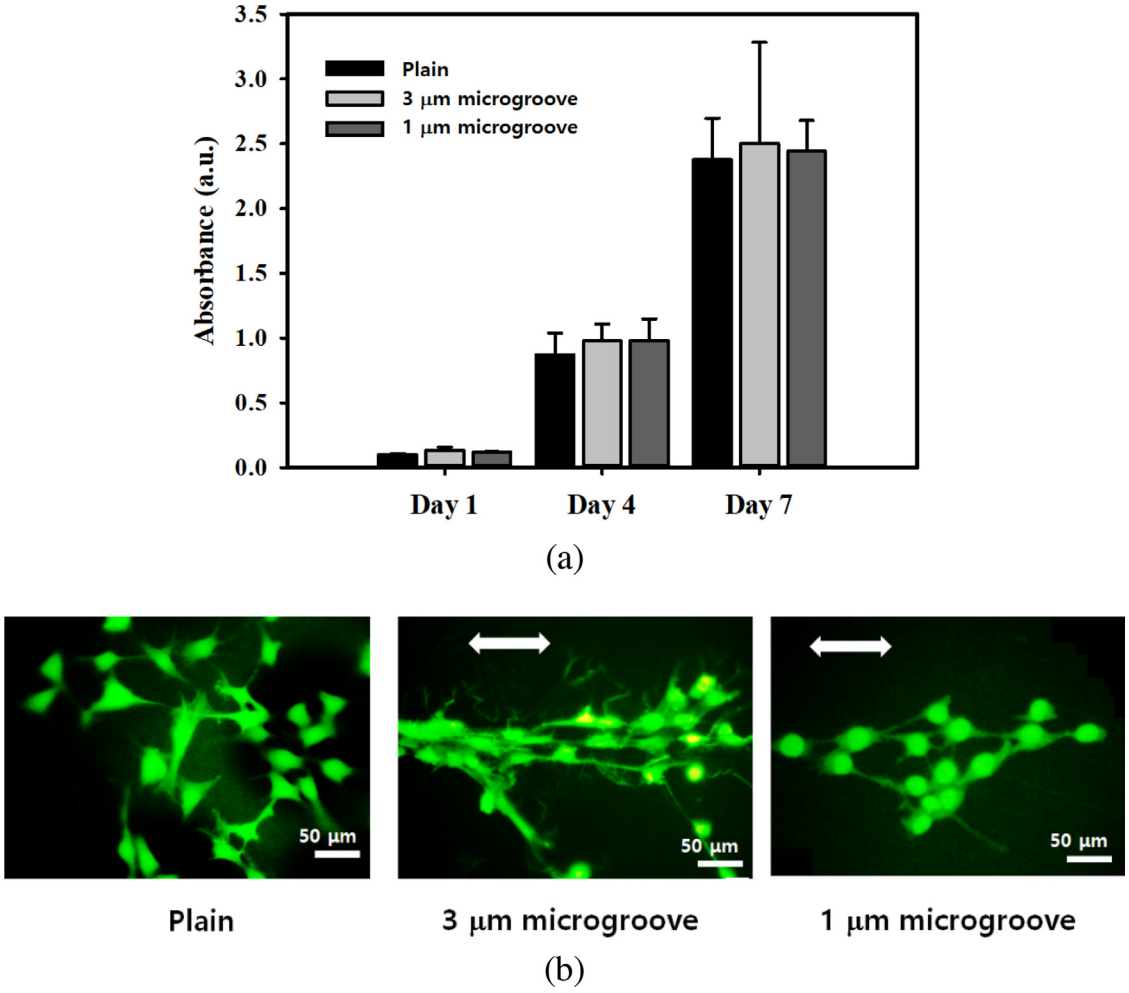

Fig. 4. (a) MTT assay and (b) fluorescence images of C2C12 obtained from live/dead fluorescence viability assay.

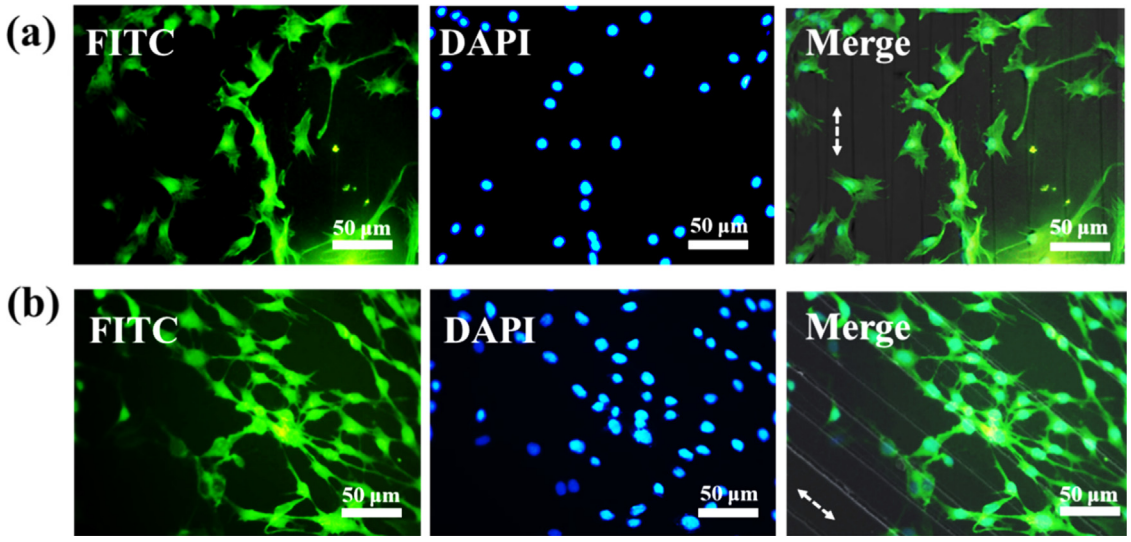

Fig. 5. Observation of C2C12 cell elongation using DAPI/FITC-phalloidin staining after 3 day culture. (a) 3 μm microgroove, (b) 1 μm microgroove.

Depending on the solubility difference, various combinations would be possible, not limited to the use of PEO fiber and PS substrates, for example, even with hydrogel substrates and hydrophobic fibers.

After successful fabrication of polymer substrates with microgroove patterns, we investigated the possibility of using them as a new platform for the topographical guidance of C2C12 myoblast cells. The C2C12 cell line, skeletal myoblast, was chosen as a model

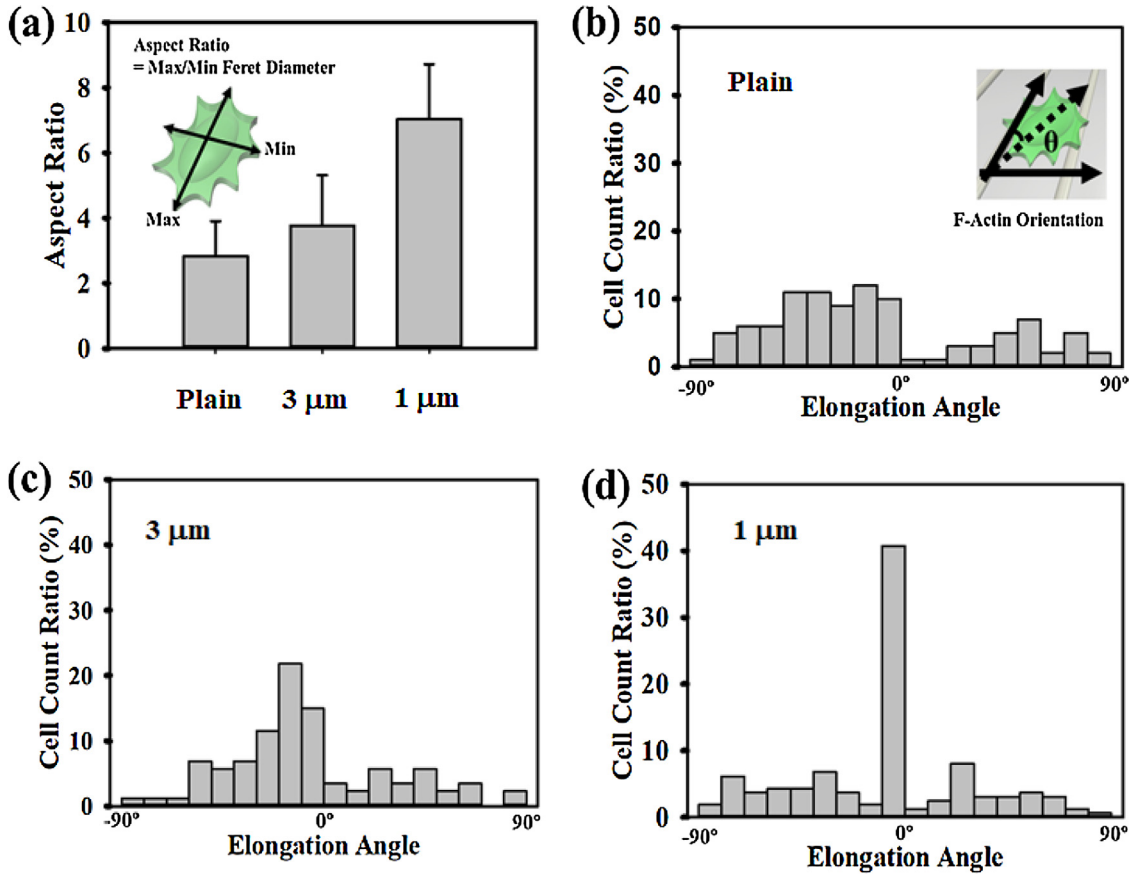

Fig. 6. (a) The plot of the aspect ratio of F-actin measured from Plain, 3 μm and 1 μm microgrooves. The plot of the alignment angles of cell bodies measured from (b) Plain, (c) 3 μm, and (d) 1 μm microgrooves.

cell because it had been shown that highly aligned patterns provided topographical cues for the alignment of C2C12, which is considered a critical step during myotube formation. Since Weiss et al. showed that cell orientation responded to surface topography, according to the concept of contact guidance, many studies have been reported on the contact guidance of various cell types using different topographic patterns [40]. Among them, groove patterns are the most common features used to achieve cell alignment. The grooved surfaces were obtained by photolithography for micrometer scales and e-beam lithography and nanoimprinting for nanometer scales, which are costly and time consuming [25,41]. Compared with those nano/microfabrication techniques, the NFEAL method is much cheaper and saves the process time dramatically. In addition, the use of harmful solvents can be minimized. Although 3D printing generates grooved substrates, their resolution is tens of micrometers while the resolution of NFEAL extends up to tens of nanometers [23].

Cytotoxicity assays revealed that the overall process to prepare grooved PS substrates was cytocompatible (Fig. 4). As a result, in the C2C12 cultures on the grooved PS supports, the interactions between the C2C12 and the underlying grooved surface were observed. C2C12 showed elongated shapes of cells along the aligned groove patterns, which were well oriented (Figs. 5 and 6). This is consistent with results of the previous studies on C2C12 cell elongation according to surface pattern [42,43]. When nano/microgroove patterns exist below the cells, the filopodia of the cells expanded directionally according to the groove pattern of the support. This is because the lamellipodia of the cells acted in the direction of expansion, moving the cells with the morphological cues of the support to induce directional cell guidance. In addition, it was confirmed that the alignment of the C2C12 cells also affected by the pattern size of the support. The directions of C2C12 cultured on the surface of the support with 1 μm microgroove showed better alignment than those cultured on a support with 3 μm microgroove. This is consistent with the results of the previous research showing that alignment increases as the width of the grooves becomes narrower [44,45], which demonstrates that the orientations of the cells can be controlled by fabricating various patterns using the NFEAL technique.

Conclusion

In this work, we prepared polymer scaffolds with microgroove patterns using the NFEAL technique. PEO fiber patterns generated by NFE were used as sacrificial fibers, whose diameters were controlled by controlling the NFE parameters such as voltage, distance, feed rate, and translation speed. As a proof of concept, diverse microscale patterns of PEO aligned fibers were fabricated by changing the NFE conditions, which showed the possibility of direct recording of fibers with controllable resolutions. The subsequent deposition of PS and the removal of PEO fiber with water successfully generated free-standing PS scaffolds with microgroove patterns. Although more fundamental biological studies are necessary, a C2C12 cell culture demonstrated that the resultant microgrooved scaffolds had good biocompatibility and that they could induce improved cell elongation and alignment. Based on these results, it is predicted that NFEAL can be widely introduced in the fabrication of new polymer-based substrate platforms for potential application in tissue engineering and biosensing. Furthermore, more complicated nano and microdevices integrating nanoscale materials can be fabricated

by combining NFEAL with conventional lithography and manufacturing.

Declaration of interest

The authors have no conflict of interest to declare.

Acknowledgements

This work was supported by the National Research Foundation of Korea (NRF) grant funded by the Korea government (MSIP) (NRF-2017M3D1A1039289 and 2018M3A9E2024583). This research was also supported by a grant from the Korea Health Technology R&D Project through the Korea Health Industry Development Institute (KHIDI), funded by the Ministry of Health & Welfare, Republic of Korea (grant number: HI18C1237 and HI15C1744)

References

[1] X.X. He, J. Zheng, G.F. Yu, M.H. You, M. Yu, X. Ning, Y.Z. Long, J. Phys. Chem. C 121 (2017) 8663.
[2] D. Sun, C. Chang, S. Li, L. Lin, Nano Lett. 6 (2006) 839.
[3] F.-L. Zhou, P.L. Hubbard, S.J. Eichhorn, G.J. Parker, Polymer 52 (2011) 3603.
[4] C. Chang, V.H. Tran, J. Wang, Y.K. Fuh, L. Lin, Nano Lett. 10 (2010) 726.
[5] Y.K. Fuh, J.C. Ye, P.C. Chen, H.C. Ho, Z.M. Huang, ACS Appl. Mater. Interfaces 7 (2015) 16923.
[6] Y.K. Fuh, S.Z. Chen, Z.Y. He, Nanoscale Res. Lett. 8 (2013) 97.
[7] Y.K. Fuh, Y.C. Wu, Z.Y. He, Z.M. Huang, W.W. Hu, Mater. Sci. Eng. C: Mater. 62 (2016) 879.
[8] T.D. Brown, P.D. Dalton, D.W. Hutmacher, Adv. Mater. 23 (2011) 5651.
[9] G. Hochleitner, T. Jungst, T.D. Brown, K. Hahn, C. Moseke, F. Jakob, P.D. Dalton, J. Groll, Biofabrication 7 (2015)035002.
[10] Z.H. Liu, C.T. Pan, C.K. Yen, L.W. Lin, J.C. Huang, C.A. Ke, Appl. Surf. Sci. 346 (2015) 291.
[11] X. Wang, G.F. Zheng, G.Q. He, J. Wei, H.Y. Liu, Y.H. Lin, J.Y. Zheng, D.H. Sun, Mater. Lett. 109 (2013) 58.
[12] G.F. Zheng, Y.B. Pei, X. Wang, J.Y. Zheng, D.H. Sun, Chin. Phys. B 23 (2014).
[13] X. Wang, G.F. Zheng, L. Xu, W. Cheng, B.L. Xu, Y.F. Huang, D.H. Sun, Appl. Phys. A: Mater. 108 (2012) 825.
[14] L. Tsai, C. Pan, C. Yen, S. Wang, A. Yang, S. Kuo, S. Wu, Z. Wen, 2017 International Conference on IEEE Applied System Innovation (ICASI), (2017) , pp. 412.
[15] Z.H. Liu, C.T. Pan, L.W. Lin, H.W. Lai, Sens. Actuators A: Phys. 193 (2013) 13.
[16] C. Chang, K. Limkrailassiri, L.W. Lin, Appl. Phys. Lett. 93 (2008)123111.
[17] G.F. Zheng, W.W. Li, X. Wang, D.Z. Wu, D.H. Sun, L.W. Lin, J. Phys. D: Appl. Phys. 43 (2010)415501.
[18] G.S. Bisht, G. Canton, A. Mirsepassi, L. Kulinsky, S. Oh, D. Dunn-Rankin, M.J. Madou, Nano Lett. 11 (2011) 1831.
[19] T. Padmanabhan, V. Kamaraj, L. Magwood, B. Starly, J. Manuf. Process. 13 (2011) 104.
[20] T.P. Lei, X.Z. Lu, F. Yang, AIP Adv. 5 (2015)041301.
[21] Z. Wang, X. Chen, J. Zeng, F. Liang, P. Wu, H. Wang, AIP Adv. 7 (2017)035310.
[22] K. Shimizu, H. Fujita, E. Nagamori, Biotechnol. Bioeng. 103 (2009) 631.
[23] R. Bhuthalingam, P.Q. Lim, S.A. Irvine, A. Agrawal, P.S. Mhaisalkar, J. An, C.K. Chua, S. Venkatraman, Int. J. Bioprinting 1 (2015) 57.
[24] C.C. Yuan, K.J. Ma, K.C. Li, H.H. Chien, H.E. Lu, C.P. Tseng, S.M. Hwang, Micro Nano Lett. 8 (2013) 440.
[25] W. Loesberg, J. Te Riet, F. Van Delft, P. Schön, C. Figdor, S. Speller, J. van Loon, X. Walboomers, J. Jansen, Biomaterials 28 (2007) 3944.
[26] J. Li, H. McNally, R. Shi, J. Biomed. Mater. Res. A 87 (2008) 392.
[27] S. Bose, S. Vahabzadeh, A. Bandyopadhyay, Mater. Today 16 (2013) 496.
[28] T.M. Patz, A. Doraiswamy, R.J. Narayan, R. Modi, D.B. Chrisey, Mater. Sci. Eng. B: Solid 123 (2005) 242.
[29] W.Y. Yeong, H. Yu, K.P. Lim, K.L. Ng, Y.C. Boey, V.S. Subbu, L.P. Tan, Tissue Eng. C: Methods 16 (2010) 1011.
[30] H. Aubin, J.W. Nichol, C.B. Hutson, H. Bae, A.L. Sieminski, D.M. Cropek, P. Akhyari, A. Khademhosseini, Biomaterials 31 (2010) 6941.
[31] M.P. Sousa, S.G. Caridade, J.F. Mano, Adv. Healthc. Mater. 6 (2017).
[32] A. Yamamoto, S. Mishima, N. Maruyama, M. Sumita, J. Biomed. Mater. Res. A 50 (2000) 114.
[33] A.S. Curtis, J.V. Forrester, C. McInnes, F. Lawrie, J. Cell Biol. 97 (1983) 1500.
[34] L. Wang, Y. Wu, B. Guo, P.X. Ma, ACS Nano 9 (2015) 9167.
[35] G.T. Christopherson, H. Song, H.Q. Mao, Biomaterials 30 (2009) 556.
[36] J.W. Xie, S.M. Willerth, X.R. Li, M.R. Macewan, A. Rader, S.E. Sakiyama-Elbert, Y. N. Xia, Biomaterials 30 (2009) 354.
[37] S.H. Lim, X.Y. Liu, H. Song, K.J. Yarema, H.Q. Mao, Biomaterials 31 (2010) 9031.
[38] Y.J. Ren, S. Zhang, R. Mi, Q. Liu, X. Zeng, M. Rao, A. Hoke, H.Q. Mao, Acta Biomater. 9 (2013) 7727.
[39] P. Fattahi, J.T. Dover, J.L. Brown, Adv. Healthc. Mater. 6 (2017).
[40] P. Weiss, J. Exp. Zool. 68 (1934) 393.
[41] L. Altomare, N. Gadegaard, L. Visai, M.C. Tanzi, S. Fare, Acta Biomater. 6 (2010) 1948.
[42] R.C. You, X.F. Li, Z.W. Luo, J. Qu, M.Z. Li, Biointerphases 10 (2015)011005.
[43] S.H. Cha, H.J. Lee, W.-G. Koh, Biomater. Res. 21 (2017) 1.
[44] J.L. Charest, A.J. García, W.P. King, Biomaterials 28 (2007) 2202.
[45] M.S. Grigola, C.L. Dyck, D.S. Babacan, D.N. Joaquin, K.J. Hsia, Biotechnol. Bioeng. 111 (2014) 1617.